

# Microstructural Analysis of Friction Welded Dissimilar Steel Joints

<sup>1</sup>Ramya Alluru, <sup>2</sup>L. Siva Rama Krishna, <sup>3</sup>P. Ravinder Reddy

*1Department of Mechanical Engineering, University College of Engineering, Osmania University, Hyderabad, Telangana, India*

*2Department of Mechanical Engineering, University College of Engineering, Osmania University, Hyderabad, Telangana, India*

*3Department of Mechanical Engineering, Chaitanya Bharathi Institute of Technology, Osmania University, Hyderabad, Telangana, India*

## Abstract

This study investigates the microstructural changes and energy-dispersive X-ray (EDX) spectra of ASTM A106 Grade B steel and EN 19 steel during friction welding, with an additional focus on the heat treatment of EN 19 steel. Friction welding, a solid-state welding process, was employed to join these two distinct steel grades, known for their differences in chemical composition and mechanical properties. The EN 19 steel underwent heat treatment prior to welding to enhance the joint's performance. Microstructural analysis is conducted using scanning electron microscopy (SEM) to observe the fusion zone, heat-affected zone (HAZ), and base material interfaces. Results indicated significant changes in grain structure and phase transformations at the weld interface, with the EN 19 steel exhibiting more pronounced refinement in the microstructure after heat treatment. EDX spectra were recorded from various regions of the welded joint to analyse the elemental distribution and identify any intermetallic phases formed due to diffusion across the interface. The analysis revealed elemental diffusion primarily in the weld region, contributing to the formation of a mixed microstructure.

*Keywords: Friction Welding, ASTM 106 grade B steel, EN 19 steel, Microstructure, Energy dispersive X-ray analysis*

## 1. Introduction

Friction welding (FW) is a solid-state welding process that utilizes mechanical friction and the heat generated by it to join materials without the need for external filler material or melting of the base metals. The process is particularly useful for joining dissimilar metals, as it minimizes the issues associated with conventional welding methods such as differences in melting points, thermal expansion, and the formation of brittle intermetallic compounds. In terms of creating lightweight structures, combining various properties into a single component, reducing overall costs, and increasing efficiency through innovative engineering solutions, dissimilar materials welding is an exceptional solution that offers several advantages [1–8]. One such combination of different materials with differences in physical, chemical, and thermal characteristics is ASTM 106 grade B steel and EN19 steel [9–13].

In the current research Friction welding of these two dissimilar metals ASTM A106 Grade B steel and EN 19 steel presents an opportunity to combine the beneficial properties of both materials in a single joint. The key challenges arise from the differences in their thermal and mechanical properties, such as thermal expansion rates, tensile strength, and hardness. However, friction welding helps to mitigate some of these issues by creating a joint that relies on the plastic deformation and diffusion at the interface of the materials rather than melting.

## 2. Experimental set up

A continuous drive friction-welding machine as shown in Fig. 1 is used to weld ASTM 106 grade B steel and EN 19 steel. The ASTM A106 Grade B and EN19 materials, which have a 200 mm outer diameter and a 10 mm pipe thickness, are used in this investigation. Table 1 displays the parent materials' chemical composition for the

purposes of this research. The input parameters taken into consideration, based on the literature, are spindle speed of 1500 rpm, friction pressure of 20 kg/cm<sup>2</sup>, forge pressure of 60 kg/cm<sup>2</sup>, friction time of 40 s, and forge time of 20 s.



**Fig 1. Continuous drive Friction Welding machine**

EN 19 steel undergoes quenching and tempering. 850 to 900°C (1562 to 1652°F) is the initial temperature at which EN 19 steel is heated. This temperature is higher than the critical temperature at which the steel changes into an austenite phase. To make sure uniform heating throughout the item, the EN 19 steel is maintained at this temperature for a predetermined amount of time. The steel is quickly chilled (quenched) in a water-quenching medium after soaking. Depending on the required mechanical qualities, the steel is warmed to a temperature usually ranging from 400 to 700°C (752 to 1292°F) after quenching. For a set amount of time, often one to two hours, the steel is kept at the tempering temperature. The steel is cooled gradually in air after soaking, which promotes the development of a more stable microstructure.

**Table 1. Chemical composition (wt %) of ASTM 106 Grade B and EN 19**

Materials	C	Mn	S	P	Si	Cr	Mo	Ni	Vn	Cu
ASTM106 Grade B	0.21	0.60	0.01	0.015	0.27	0.057	0.014	0.007	0.001	0.017
AISI 4140	0.35-0.45	0.5-0.8	0.05	0.05	0.10-0.35	0.9-1.5	0.2-0.4	-----	-----	-----

### 3. Results and Discussions

Microstructural analysis of friction-welded ASTM A106 Grade B steel and EN19 steel, both with and without heat treatment of the EN19 steel, involves examining the grain structure & phase composition of the weld zones and base materials. The Figure 2 (a) comprises of Ferrite and pearlite microstructure. The primary constituents of steel's ferrite phase are iron and a trace amount of carbon (less than 0.02% by weight). The crystal structure of ferrite is body-centered cubic (BCC). Relatively soft and ductile, ferrite occurs with lower carbon concentrations. Pearlite is a lamellar (alternating layer) structure composed of cementite (Fe<sub>3</sub>C) and ferrite that is formed when steel is cooled gradually through the eutectoid temperature (about 727°C) of the iron-carbon phase diagram. It has about 0.8% carbon by weight and provides a nice mix of toughness and strength. Because of its chemical composition, cooling rates, and heat treatment procedures, ASTM A106 Grade B (a carbon steel used for high-

temperature and high-pressure applications) and EN 19 (a medium carbon alloy steel) frequently develop ferrite and pearlite microstructures. About 0.40 % carbon is present in EN 19, an alloy steel that also contains nickel (Ni) and chromium (Cr). While the other components aid in enhancing the hardenability and general mechanical qualities, the carbon content permits the creation of pearlite. EN 19 forms a mixture of ferrite and pearlite because the steel is cooled at rates that allow these phases to stabilize.

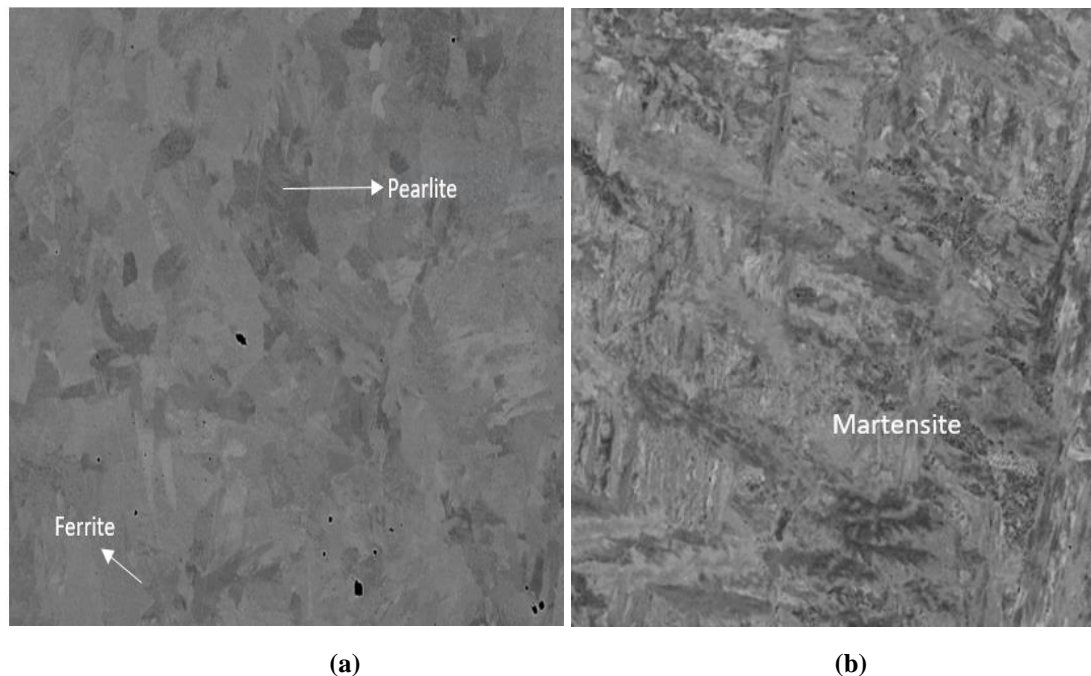


**Fig. 2 Microstructure of a) ASTM 106 grade B steel and (b) Heat treated EN 19 steel**

ASTM A106 Grade B steel contains a carbon content of about 0.26%. This amount of carbon tends to cause the microstructure to cool and create a mixture of pearlite and ferrite. Similar to EN 19, ferrite forms as the major phase and pearlite forms at the eutectoid temperature due to the cooling rate and chemical composition. The amount of carbon content plays a key role in the formation of pearlite structure. For ASTM A106 Grade B (with roughly 0.26% carbon) and EN 19 (with roughly 0.40% carbon), the steel has enough carbon to permit the formation of pearlite during slow cooling, but not enough to form phases like martensite (which require higher carbon content and rapid cooling).

From Fig. 2 (b) A phase transformation called Martensite is formed because the cooling rate is faster than the equilibrium transformation rate. Martensite is hard and brittle due to the distorted lattice created by the carbon atoms, which restrict the movement of dislocations. The carbon content in EN 19 steel is high enough to allow for the formation of martensite. The higher the carbon content, the more martensite can form, and harder the steel will be. The hardness of the martensite can be controlled through the quenching process and subsequent tempering in order to reduce brittleness.

The Fig. 3(a) image shows a microstructure of austenite, also known as gamma-iron, which is an iron alloy formed by heating iron and other elements between 723 and 1500 °C. Atoms are located in the center of each face and at each corner of the cube, giving it a face centered cubic crystal lattice structure. Since pure austenite is unstable outside of a certain temperature range, austenite will remain stable at ambient temperature as long as nickel is present. Due to the rapid cooling during quenching, which prevents full transformation to martensite, a small amount of austenite, known as "retained austenite," may be present in the microstructure of EN 19 steel after it has undergone a quenching and tempering heat treatment. Tempering then stabilizes this retained austenite, preventing its full decomposition into other phases. The subsequent tempering process, which involves reheating at a lower temperature, can further stabilize the retained austenite by allowing carbon atoms to redistribute within the lattice.

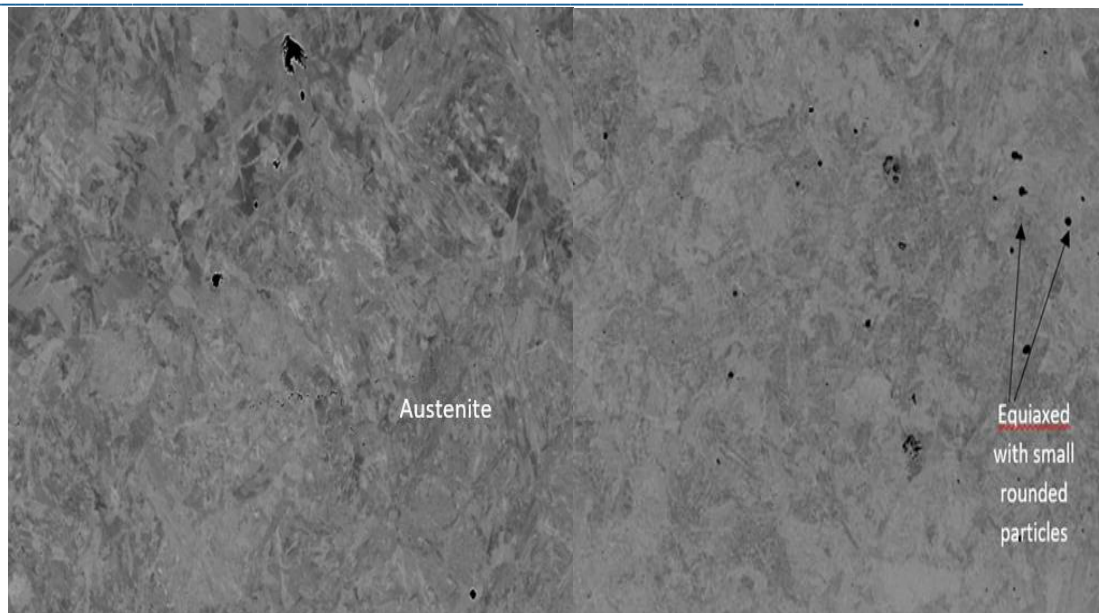


**Fig. 3 a) Microstructure of Austenite and b) Formation of intermetallics at weld interface**

**Intermetallic Formation:** In the case of dissimilar materials ASTM A106 Grade B and EN 19 steel, the formation of intermetallics can occur. These typically brittle compounds form at the interface due to the diffusion of elements from one material to another. The interface contains intermetallic phases such as iron (Fe), carbon (C), chromium (Cr), and molybdenum (Mo) from the respective materials.

**Interface Microstructure:** ASTM A106 Grade B steel (carbon steel) will primarily consist of ferrite and pearlite in its base microstructure. EN 19 steel has a martensitic structure in its quenched state due to its higher carbon and alloy content. During friction welding, the region near the weld interface can undergo tempering or even some phase transformation to form a more tempered martensite structure, especially at higher welding temperatures.

**Weld Zone:** In the weld zone, a complex mix of Martensitic structures formed due to rapid cooling in high-carbon steel areas and tempered martensitic phases, where carbide formation and the diffusion of alloying elements like Mo and Cr into the adjacent regions occur. Intermetallic phases at the interface that are generally brittle and weak compared to the base materials. These are typically undesirable but may form if the friction welding parameters are not optimized.

In Fig. 3 (b) microstructure, intermetallics are created at the weld interface of ASTM 106 grade B steel and EN 19 steel. An equiaxed shape with tiny spherical particles dispersed throughout the matrix. Because of the heat produced at the interface, both materials experience substantial microstructural changes during friction welding. Although the localized temperatures can be high enough to induce phase changes, diffusion, and the creation of tiny intermetallic compounds, as the friction welding process usually takes place below the melting point.

#### **Energy Dispersive X- Ray Analysis (EDXA)**

The heat treatment of EN19 steel typically involves processes like quenching and tempering, which improve its hardness, tensile strength, and wear resistance. These treatments alter the microstructure, primarily by transforming the steel's pearlite and ferrite structure into martensite, depending on the cooling rates and temperatures used. When EN19 is heat-treated, it will show higher hardness and might undergo changes in elemental composition, especially in the phase distribution in the microstructure, which could be visible in the EDX analysis.

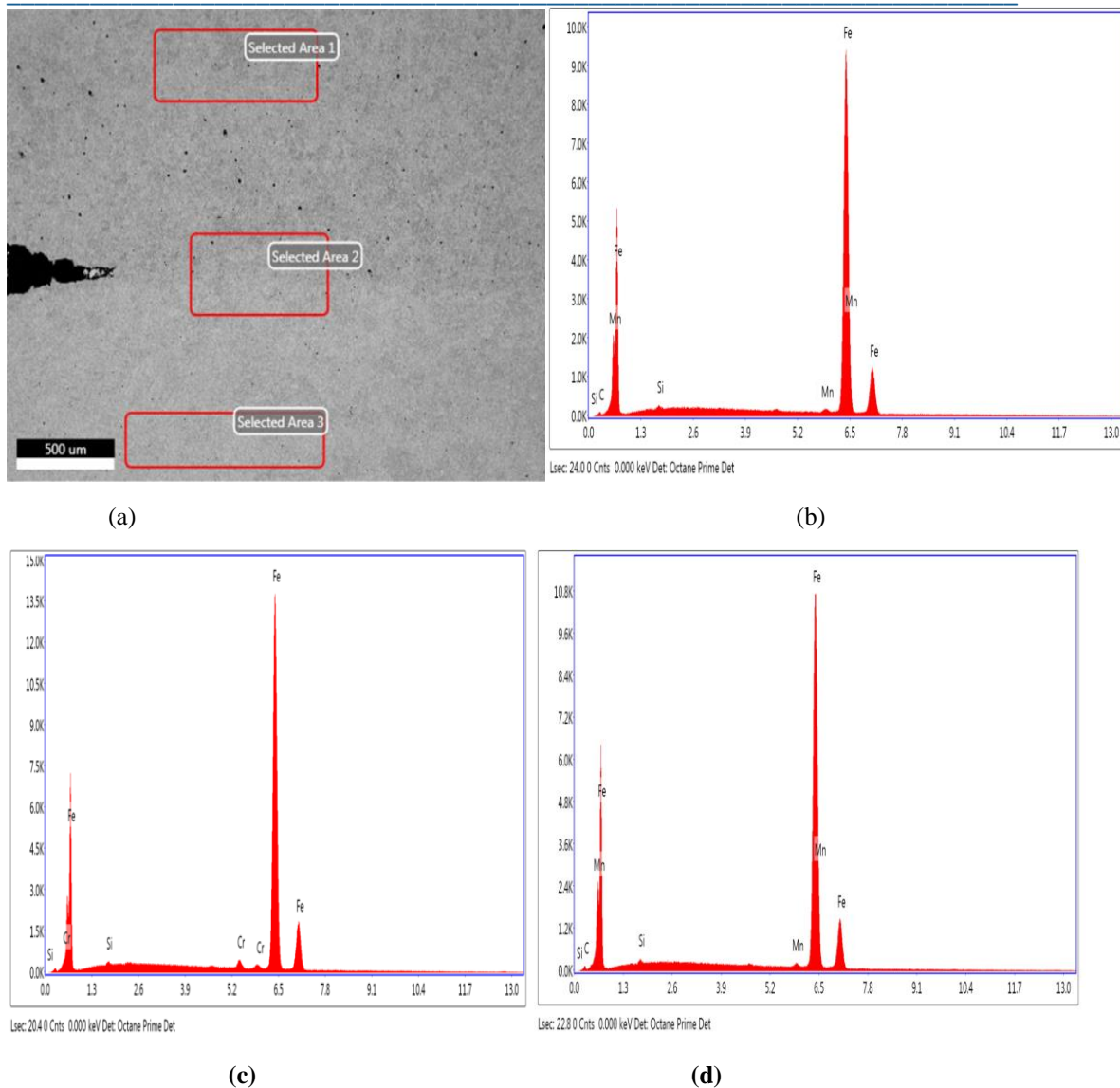


**Fig. 4 (a), (b), (c), (d) EDX Spectra at Heat affected zone and weld interface**

As illustrated in the fig. 4 (a), (b), (c) & (d) under EN 19 steel heat treatment conditions, spectroscopic analysis of the friction-welded EN 19 steel and ASTM A 106 Grade B steel pipes was carried out in the vicinity of the weld interface region to characterize the solid-state diffusion of carbon, manganese, and chromium silicon atoms across the weld joint of C, Mn at the weld interface. A considerable flow of chromium and carbon seems to occur from adjacent regions to the interface region. The contact has thus been obviously enhanced in chromium and carbon. The considerable frictional heat generated during welding seems to have facilitated the diffusion of C, Mn, and Cr towards the weld interface. Here are several distinct stages

**Phase Distribution:** Because of frictional heating, phase alterations may take place in the heat-affected zone (HAZ). Phases like ferrite, pearlite, or martensite may occur as a result of the carbon concentration, affecting the weld's mechanical characteristics. EDX can assist identify these phases by their distinct elemental signatures.

**Intermetallic Phases:** The occurrence of intermetallic phases at the weld interface may result from the presence of nickel, chromium, and other alloying components. This might have an impact on the joint's overall performance. These stages are frequently fragile and, if not adequately managed, might weaken the weld.

**Heat-Affected Zone (HAZ) - EDX examination** can reveal any compositional deviations in the HAZ, where the steel may experience microstructural alterations. There is a gradient in alloying elements due to diffusion over the

border between the two steels. For instance, the presence of nickel and chromium from the EN 19 side can produce localized hardness.

**Inter diffusion Zone** - There could be inter-diffusion of elements at the interface, particularly carbon, manganese, chromium, and nickel. This region will show mixed elemental distributions, where elements from both materials diffuse into each other due to the high temperature generated during welding.

### Conclusion

The weld zone at the interface could show a gradient of microstructures due to the difference in thermal histories of the two materials. For ASTM 106 Grade B steel, a relatively ferritic structure is formed, while the EN 19 steel could show more refined martensitic or tempered martensitic structures depending on the heat treatment applied. The bonding interface has shown some evidence of phase transformations, such as the formation of ferrite and pearlite in ASTM 106 Grade B steel and martensite in EN 19 steel.

### References

1. Aritoshi M, Okita K. Friction welding of dissimilar metals. *Weld Int* 2003;17:271–5.
2. [2] Meshram SD, Mohandas T, Reddy GM. Friction welding of dissimilar pure metals. *J Mater Process Technol* 2007;184:330–7.
3. [3] Mehta KP, Badheka VJ. A review on dissimilar friction stir welding of copper to aluminum: process, properties, and variants. *Mater Manuf Process* 2016;31: 233–54.
4. [4] Mehta KP. A review on friction-based joining of dissimilar aluminum-steel joints. *J Mater Res* 2019;34:78–96.
5. [5] Uzkut M, Ünlü B, Yılmaz S, Akdağ M. Friction welding and its applications in Today's world. *Sarajev Int Symp Sustain Dev* 2010:710–24.
6. [6] Uday MB, Fauzi MNA, Zuhailawati H, Ismail AB. Advances in friction welding process: a review. *Sci Technol Weld Join* 2010;15:534–58.
7. [7] Peng H, Chen C, Zhang H, Ran X. Recent development of improved clinching process. *Int J Adv Manuf Technol* 2020;110:3169–99.
8. [8] Gao P, Zhang Y, Mehta KP. Metallurgical and mechanical properties of Al–Cu joint by friction stir spot welding and modified friction stir clinching. *Met Mater Int* 2020.
9. [9] Shanjeevi C, Kumar SS, Sathiya P. Multi-objective optimization of friction welding parameters in AISI 304L austenitic stainless steel and copper joints. *Proc Inst Mech Eng Part B J Eng Manuf* 2016;230:449–457.
10. [10] Sahin M. Joining of stainless steel and copper materials with friction welding. *Ind Lubr Tribol* 2009;61:319–24.
11. [11] Li Y, Chen C, Yi R, Ouyang Y. Review: special brazing and soldering. *J Manuf Process* 2020;60: 608–35.
12. [12] Han J, Paidar M, Vignesh RV, Mehta KP, Heidarzadeh A, Ojo OO. Effect of shoulder features during friction spot extrusion welding of 2024-T3 to 6061-T6 aluminium
13. [13] Kumar D, Kore SD, Nandy A. Finite element modeling of electromagnetic crimping of Cu-SS tube-to-tube joint along with simulation of destructive testing for strength prediction of the joint. *J Manuf Sci Eng* 2021;143:1–11.